Since January 2020 Elsevier has created a COVID-19 resource centre with free information in English and Mandarin on the novel coronavirus COVID-19. The COVID-19 resource centre is hosted on Elsevier Connect, the company's public news and information website.

Available online at www.sciencedirect.com
ScienceDirect
Journal of Structural Biology 155 (2006) 162–175
Journal of Structural Biology
www.elsevier.com/locate/yjsbi

Biophysical characterization of HRC peptide analogs interaction with heptad repeat regions of the SARS-coronavirus Spike fusion protein core

Zhe Yan, Brian Tripet, Robert S. Hodges *

Department of Biochemistry and Molecular Genetics, University of Colorado at Denver and Health Sciences Center, Aurora, CO 80045, USA

Received 30 January 2006; accepted 23 March 2006
Available online 27 April 2006

Abstract

The Spike (S) protein of SARS-coronavirus (SARS-CoV) mediates viral entry into host cells. It contains two heptad repeat regions, denoted HRN and HRC. We have identified the location of the two interacting HR regions that form the six-helix bundle (B. Tripet, et al, J. Biol. Chem., 279: 20836–20849, 2004). In this study, HRC peptide (1150–1185) was chosen as the region to make structure-based substitutions to design a series of HRC analogs with increased hydrophobicity, helical propensity and electrostatic interactions, or with a covalent constraint (lactam bridge) to stabilize the α-helical conformation. Effects of the substitutions on α-helical structure of HRC peptides and their abilities to interact with HRN or HRC have been examined by biophysical techniques. Our results show that the binding of the HRC analogs to HRN does not correlate with the coiled-coil stability of the HRC analogs, but their interactions with HRC does correlate with their stability, except for HRC7. This study also suggested three types of potential peptide inhibitors against viral entry can be designed, those that simultaneously inhibit interaction with HRC and HRN and those that are either HRC-specific or HRN-specific. For example, our study shows the important role of α-helical structure in the formation of the six-helix bundle where the lactam bridge constrained analog (HRC5) provided the best interaction with HRN. The importance of α-helical structure in the interaction with native HRC was demonstrated with analog HRC4 which binds best to HRC.

Keywords: Severe acute respiratory syndrome (SARS); Coronavirus (CoV); SARS-CoV; Spike protein; Heptad repeat regions (HRN and HRC); Coiled-coil; Six-helix bundle state

1. Introduction

Severe acute respiratory syndrome (SARS) is an acute respiratory illness caused by infection with a novel coronavirus (SARS-CoV). The severity and mortality of this illness was witnessed during the global pandemic of SARS-CoV in 2003. The virus has not re-emerged since July 2003, except for several cases of laboratory-acquired infections and one natural outbreak resulting in four infected people (Normile, 2004a; Normile, 2004b). However, since SARS-CoV-related viruses have been detected in some animals, it still remains a threat due to its highly transmittable nature to human populations and the mysterious origin of SARS-CoV (Guan et al., 2003; Hartley and Smith, 2003). Currently, since there is no effective agent for the anti-viral therapy of SARS-CoV infection, it is imperative to learn as much as possible about this virus to accelerate the development of therapeutics and vaccines for its re-emergence.

Infection by SARS coronavirus requires fusion of the viral and cellular membranes, which is mediated by the viral envelope Spike (S) glycoprotein and receptors on the target cell (Holmes, 2005). The S protein is a type I viral fusion protein which contains two highly conserved heptad repeat (HR) domains that have been shown to form coiled-coil structures (Bosch et al., 2003; Hakansson-McReynolds et al., 2006; Spaan et al., 1988; Tripet et al., 2004). The HR

* Corresponding author. Fax: +1 303 724 3249.
E-mail address: Robert.hodges@uchsc.edu (R.S. Hodges).

1047-8477/$ - see front matter © 2006 Elsevier Inc. All rights reserved.
doi:10.1016/j.jsb.2006.03.024

region located closest to the N-terminus in the sequence is denoted HRN and the HR region located closest to the C-terminus is denoted HRC. Although the exact mechanism by which the SARS-CoV enters the host cell has not been elucidated, it is most likely similar to other coronaviruses. Upon binding to the receptor at the cell membrane, the fusion protein will be induced into the fusogenic intermediate state with a dramatic conformation change. Collapse of this fusogenic intermediate leads to a six-helix bundle (trimer of dimers) formation between HRN and HRC, which ultimately promotes membrane fusion (Eckert and Kim, 2001b). Our laboratory and other researchers recently reported (Bosch et al., 2004; Ingallinella et al., 2004; Tripet et al., 2004; Xu et al., 2004b) that HR regions of SARS-CoV S protein can associate to form a very stable α-helical six-stranded structure and the orientation of the HR regions is anti-parallel. Residues 902–950 in the HRN region and 1151–1185 in the HRC region were identified to be crucial for their interaction. The structure of the ectodomain of SARS Spike protein in its fusogenic/post-fusogenic state and HR interaction regions have recently been confirmed by crystallography (Duquerroy et al., 2005; Supekar et al., 2004; Xu et al., 2004a). Most recently, Li et al. (2005) reported the crystal structure of the SARS-CoV S receptor binding domain (residues 306–575) complexed with receptor ACE2 (angiotensin-converting enzyme 2), which further confirms the prediction that SARS-CoV fusion process is similar to other viruses with type I fusion proteins. Hakansson-McReynolds et al. (2006) also reported the solution structure of the SARS-Coronavirus HRC domain (1143–1193) in the prefusion state, which forms a coiled-coil symmetric trimer.

A critical step in viral entry is the conformational change of the fusion domain of the S protein. Peptides derived from the HRC region of the HIV-1 gp41 and other class I fusion proteins have been reported to show significant viral fusion inhibitory activity (Chan and Kim, 1998; Eckert and Kim, 2001a; Root et al., 2001). It has been proposed that HRC analogs bind strongly to the transiently exposed HRN coiled-coil trimer, and block the formation of the six-helical bundle necessary for the fusion. For HIV and murine CoV mouse hepatitis virus (MHV), HRC peptides have been shown to inhibit viral entry at nanomolar concentrations (Bosch et al., 2004; Chan and Kim, 1998). Recently, a HIV peptide inhibitor has been made by the fusion of gp41 HRN region and a trimeric forming coiled-coil peptide, where the three chains are covalently linked by disulfide bridges. This construct was a potent inhibitor of viral entry at pM concentration (Bianchi et al., 2005). One of the HRC peptides of HIV-1 gp41, Enfuvirtide (Fuzeon), was approved by the FDA for treatment of AIDS (LaBonte et al., 2003). In several recent studies (Bosch et al., 2004; Liu et al., 2004; Yuan et al., 2004; Zhu et al., 2004), SARS-CoV S-mediated fusion was shown to be inhibited by HRC-derived peptides; however, these peptides inhibited viral entry at concentrations in the micromolar range (Bosch et al., 2004; Liu et al., 2004). One possible reason for the higher inhibitory concentration is that the interaction between the inhibitory peptides and HRN or HRC is too weak to prevent the native intra-molecular association of HRN and HRC. As reported in studies of HIV peptide inhibitors, considerable genetic and biophysical evidence supports the concept that the ability of the Class I envelope glycoprotein to mediate membrane fusion is determined, in part, by the high stability of the six-helix bundle (Eckert and Kim, 2001b; Skehel and Wiley, 2000). Thus, peptides inhibiting the fusion process must be designed with the highest binding affinity/stability to be useful for preventing viral entry.

In the present study, HRC peptide (1150–1185) was chosen as the region to make structure-based substitutions to design a series of HRC analogs. These HRC analogs were designed with increased hydrophobicity, helical propensity and electrostatic interactions, or with a covalent constraint (lactam bridge) to stabilize the α-helical structure. Effects of the substitutions on the conformation of HRC peptides and their abilities to interact with HRN or HRC have been examined by biophysical techniques.

2. Materials and methods

2.1. Preparation of peptides

2.1.1. Peptide synthesis

The HRN and HRC peptides of SARS-CoVS glycoprotein were prepared by solid-phase synthesis methodology-using 4-benzylhydrylamine hydrochloride resin with conventional *fmoc* (fluorenylmethoxycarbonyl) chemistry as described by Tripet et al. (2000).

The synthesis of the covalent HRC trimer and HRN trimer for surface plasmon resonance analysis was carried out as described by Tripet et al. (2006).

The gene sequence Gene bank Accession No. for the SARS-CoV S protein is AY278741.

2.1.2. Lactam formation on peptide resin

The protecting groups for the side-chains of Lys1170 and Glu1166 in the HRC5 sequence which forms the *i*, *i* + 4 lactam bridge were the allyloxycarbonyl group (Aloc) for Lys and the allylester for Glu, Glu (OAl). These two protecting groups were removed by Tetrakis(triphenylphosphine)palladium(0) [$Pd(PPh_3)_4$] as described by Kates et al. (1993). The reaction was carried our under argon. Formation of the lactam ring was achieved with benzotriazole-1-yl-oxy-tris(pyrrolidino)phosphonium hexafluorophosphate (pyBOP) in the presence of *N*,*N*-diisopropylethylamine (DIEA).

2.1.3. Peptide purification and characterization

Peptides were N-terminally acetylated, cleaved from the-resin, and purified by reversed-phase high-performance liquid chromatography (RP-HPLC) on a Zorbax 300 SB-C8 preparative column (250 mm × 9.4 mm I.D., 6.5 μm particle size, 300-Å pore size; Agilent Technologies, Little Falls,

DE) with a linear AB gradient (0.6% B/min) at a flow rate of 2 ml/min, where eluent A is aqueous 0.05% trifluoroacetic acid (TFA) and eluent B is 0.05% TFA in acetonitrile. Homogeneity of the purified peptides was characterized by analytical RP-HPLC, amino acid analysis, and electrospray mass spectrometry.

2.2. Circular dichroism spectroscopy

Circular dichroism spectra were recorded on a Jasco J-810 spectropolarimeter (Jasco Inc., Easton, MD). The CD wavelength scans were measured from 190 to 255 nm in benign buffer (0.1 M KCl, 0.05 M PO_4, pH 7.0). For samples containing trifluoroethanol (TFE), the above buffer was diluted1:1 (v/v) with TFE. Temperature denaturation midpoints (T_m) for the peptides were determined by following the change in molar ellipticity at 222 nm from 4 to 95 °C in a 5-mm path length cell and a temperature increase rate of 1 °C/min. Ellipticity readings were normalized to the fraction of peptide folded (f_f) or unfolded (f_u) using the standard equations $f_f = ([\theta] - [\theta]_u)/([\theta]_n - [\theta]_u)$ and $f_u = (1 - f_f)$; where $[\theta]_n$ and $[\theta]_u$ represent the molar ellipticity values for the native fully folded and fully unfolded species, respectively. $[\theta]$ is the observed molar ellipticity at 222 nm at any temperature.

2.3. Size-exclusion and reversed-phase HPLC

HRN and HRC peptides singly or as an equimolar mixture (200 μM of each peptide) were dissolved in 100 mM KCl, 50 mM PO_4 buffer, pH 7, and equilibrated at room temperature for 30 min. A 10-μl aliquot of sample was analyzed with a high-performance size-exclusion column, Superdex 75™ (30 cm × 1 cm I.D., Amersham Biosciences, Uppsala, Sweden) equilibrated in a buffer consisting of 50 mM sodium phosphate/150 mM NaCl, pH 7.5, at a flow rate of 0.5 ml/min and ambient temperature. The molecular weights of the peak fractions were estimated by comparison with a protein standard running on the same column.

For peptides that formed stable hetero-stranded complexes, the complex peak was collected and analyzed by RP-HPLC on an analytical C8 column (Zorbax 300SB-C8, 150 mm × 4.6 mm I.D, 6.5 μm particle size, 300-Å pore size). The peptides were eluted from the column by employing a linear AB gradient of 2% B/min, where eluent A is 0.05% aqueous TFA and eluent B is 0.05% TFA in acetonitrile at a flow rate of 1.0 ml/min at room temperature.

2.4. Native-polyacrylamide gel-electrophoresis (PAGE)

Equimolar mixtures (200 μM of each peptide) of HRN (in phosphate buffer, pH 7.3) and each HRC analog were incubated at 25 °C for 10 min (sample volume was 5 μl). After the addition of an equal volume of 2 × native sample buffer (0.125 M Tris · HCl, pH 6.8/10% glycerol/0.004 g of bromophenol blue) the mixture was analyzed by PAGE on a 15% Tricine gel with a Tricine/glycine running buffer (pH 8.3). Gel electrophoresis was carried out with 120 V constant voltage at 4 °C for 2 h. The gel was then stained with Coomassie blue.

2.5. Surface plasmon resonance (SPR) analysis

To measure the binding affinity or kinetic dissociation constant of the SARS-CoV related peptides, we used surface plasmon resonance with an optical biosensor (model BIACORE 3000, BIACORE Inc, Piscataway, NJ, USA).

Covalent coupling of HRN trimer or HRC trimer to the BIACORE CM5 chip (a dextran-coated sensor chip) surface was performed following the standard amine coupling procedure according to the manufacturer's specification. Briefly, the dextran surface of the CM5 chip was first activated with 20 μl *N*-hydroxysuccinimide (NHS)/*N*-ethyl-*N*′-(dimethyl-aminopropyl)-carbodiimide (EDC). HRN trimer or HRC trimer in 10 mM sodium acetate buffer (pH4.3) was injected and allowed to react to give a surface density of 420 resonance units (RU) for the HRC trimer chip and 2000 RU for the HRN chip. Remaining activated groups were then blocked by injection of 35 μl ethanolamine HCl. A reference surface with the same treatment except no injection of ligand was generated at the same time and was used as background to correct instrument and buffer artifacts.

Binding experiments were performed at 25 °C in PBS buffer, pH 7.4, with 0.005% Tween 20. The peptides to be tested were introduced at four serial concentrations (5, 10, 20, and 50 μM) in running buffer in 80 μl injection volumes and at a flow rate of 20 μl/min, followed by 6 min of dissociation. Each experiment was carried out at least three times. Remaining analytes were removed in the surface regeneration step using 6 M guanidine hydrochloride in 20 mM glycine, pH 2.0 for the HRN trimer chip, and 100 mM acetate buffer, pH 4.0 for the HRC trimer chip.

In Tables 2 and 4, the K_{on} and K_{off} values could not determined since the simple 1:1 binding model could not be used to fit the observed data. The results are complicated by the fact that the HRC analog flowing over the chip surface is in a monomer–oligomer equilibrium and the binding event on the immobilized HRC trimer or HRN trimer could involve the binding of one or more HRC polypeptide chains. At present no model is available to calculate these parameters for such a complex system. Thus, a simple "+" or "−" was used to denote binding or no binding, respectively.

3. Results

3.1. Peptide design

Residues 902–950 in the HRN region and 1150–1185 in the HRC region were identified to be crucial for their interaction to form the six-helix bundle state (Bosch et al., 2004; Ingallinella et al., 2004; Tripet et al., 2004; Xu et al., 2004b). Furthermore, it has been reported that SARS-CoV S-mediated fusion can be inhibited in a concentration-dependent

manner by HRC-derived peptides in this HRC region (Liu et al., 2004; Zhu et al., 2004). Therefore, in our study, the 36-residue HRC peptide (1150–1185) was chosen as the region to make structure-based substitutions to design a series of HRC analogs, to increase coiled-coil stability and their ability to interact with HRN (902–950) or HRC (1150–1185) (Fig. 1).

In the design of peptide inhibitors, one must consider the following: first, in the current model of membrane fusion, the anti-viral activity of peptide fusion inhibitors would depend on the binding affinity between the peptide and the HRN region or HRC region of SARS-CoV S2. Second, substitutions in the peptide sequence to change its conformation or stability could substantially affect the interaction with the target (HRN or HRC) (Chan et al., 1998; Eckert and Kim, 2001a; Lu et al., 1995). For example, the HRC region was shown to have α-helical structure on its own (Hakansson-McReynolds et al., 2006; Tripet et al., 2004), suggesting that enhancement of α-helical structure and stability could increase affinity of potential peptide inhibitors for their helical targets. Factors that contribute to the helical conformation of peptides and stability of coiled-coils have been systematically studied (Chakrabartty et al., 1994; Houston et al., 1995; Houston et al., 1996; O'Neil and DeGrado, 1990; Tripet et al., 2000; Wagschal et al., 1999b; Zhou et al., 1994). There are two general ways to stabilize the coiled-coil. Increasing the hydrophobicity of the residues in the hydrophobic core stabilizes the coiled-coil (Tripet et al., 2000; Wagschal et al., 1999b) or increasing interactions that stabilize the individual α-helix (increasing α-helical propensity of residues, adding intra-chain electrostatics or intra-chain covalent constraints) which in turn stabilizes the coiled-coil by shifting the monomer-trimer equilibrium in favor of the folded trimeric coiled-coil. Thus, we designed the substitutions shown in Fig. 1 which involved:

(1) Increasing hydrophobicity in the hydrophobic core: (HRC1).
(2) Increasing helical propensity (HRC2 and HRC4).
(3) Increasing hydrophobicity in the hydrophobic core and increasing helical propensity (HRC3).
(4) Introducing an i to $i+4$ lactam bridge (HRC5).
(5) Introducing intrachain i to $i+3$ or i to $i+4$ salt bridges (HRC6 and HRC7).

3.2. Circular dichroism analysis of HRC analogs

To examine the change in α-helical structure of the HRC analogs, we analyzed each peptide by circular dichroism spectroscopy (CD). As seen in Fig. 3, under physiological conditions, all of these analogs are well folded, soluble, and have typical α-helical spectra.

The content of α-helicity of the native HRC peptide was concentration-dependent. It appeared to be largely unfolded at low concentrations (26% helix at 7 μM), while at 70 μM it was 65% α-helical (Fig. 2 and Table 1). It was previously shown by sedimentation equilibrium experiments that HRC forms a trimer in the analytical

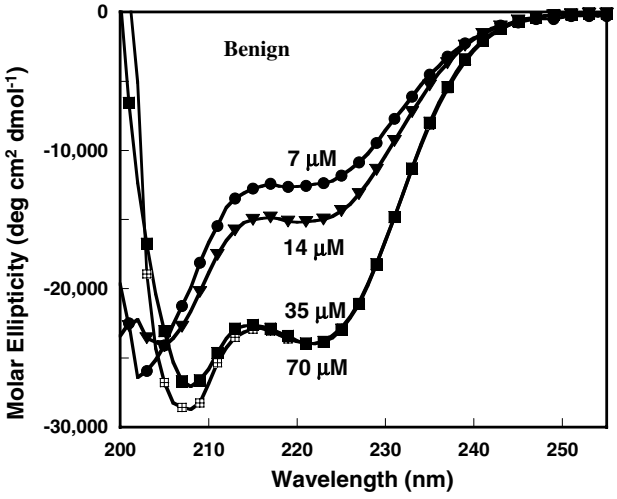

Fig. 2. CD spectra of native HRC (1150–1185) at different concentrations. Spectra were recorded in a 0.1 M KCl, 0.05 M PO_4 buffer, pH 7.

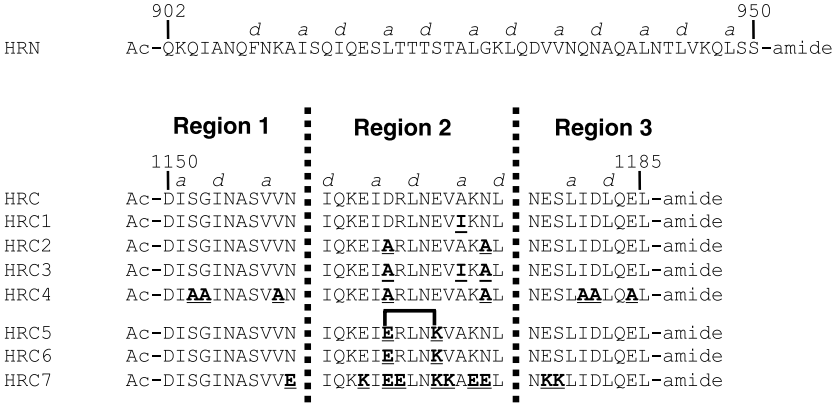

Fig. 1. Amino acid sequences of peptides used in the study. The *a* and *d* positions of the predicted coiled-coil heptad repeats (*abcdefg*)*n* are shown above the sequence. HRC1−HRC7 are HRC-derived peptides, where the residues in bold and underlined are substitutions in the native HRC (1150–1185) sequence. The HRC sequence was divided into 3 regions based on the three-dimensional structure of HRC in the six-helix bundle state, Region 1 and 3 are extended in the structure and Region 2 is α-helical.

Table 1
Ellipticity and stability of the synthetic peptides

Peptide name	$[\theta]_{222}$[a]		% α-helix[b]		$[\theta]_{222/208}$		T_m[c] (°C)	Oligomerization state[d]
	Benign	50% TFE	Benign	50% TFE	Benign	50% TFE		
HRC	−21 370	−29 720	65	91	0.86	0.85	37	Trimer
HRC 1	−32 060	−31 510	98	96	0.97	0.86	57	Tetramer
HRC 2	−27 060	−29 740	83	91	0.93	0.85	48	Trimer
HRC 3	−30 900	−31 450	95	96	0.98	0.86	66	Tetramer
HRC 4	−28 560	−30 990	87	95	1.09	0.90	74	Tetramer
HRC 5	−27 770	−32 320	85	99	0.87	0.86	41	Trimer
HRC 6	−16 510	−30 190	51	92	0.79	0.84	32	Trimer
HRC 7	−32 440	−32 660	99	100	1.01	0.88	61	Trimer

[a] $[\theta]_{222}$ is the mean residue molar ellipticity (degrees $cm^2\ dmol^{-1}$) measured at 222 nm in a 0.1 M KCl, 0.05 M PO_4 buffer, pH 7, in the absence (Benign) or presence of 50% trifluoroethanol (50% TFE) (v/v). Concentration of peptides was 70 μM.
[b] The ellipticity value in 50% TFE for peptide HRC7 was taken as 100% and % α-helical content of the other peptides were relative to HRC7.
[c] T_m is the temperature at which there is a 50% decrease in α-helical content compared to the fully folded coiled-coil as determined by circular dichroism spectroscopy at 5 °C.
[d] Oligomerization state of peptides was determined by SEC-HPLC. Concentration of peptides was 100 μM.

ultracentrifuge (Tripet et al., 2004). The CD results agree with a monomer-trimer equilibrium at low concentrations and a fully-folded trimer state occurring at 70 μM. Thus, the HRC peptide does not form a very stable oligomer.

As illustrated in Fig. 3 and Table 1, the HRC analogs had a higher content of helical structure compared to HRC, except for HRC6 which was designed as the control peptide for HRC5 and HRC7, showed lower helical structure than native HRC. HRC1, HRC3, and HRC7 are essentially fully folded in benign buffer (>95% α-helical content, Table 1) and thus no significant change in helical structure is observed by addition of the helix inducing solvent, TFE. However, HRC and HRC6 were not fully folded in benign buffer and substantial α-helical structure could be induced by addition of TFE.

To test the stability of the HRC analogs, each analog was denatured by increasing temperature, as illustrated in Fig. 4, and their T_m values are shown in Table 1. These results showed that all analogs were more stable than native HRC, as expected, except for HRC6, which was less stable than native HRC (T_m values range from 32 to 74 °C).

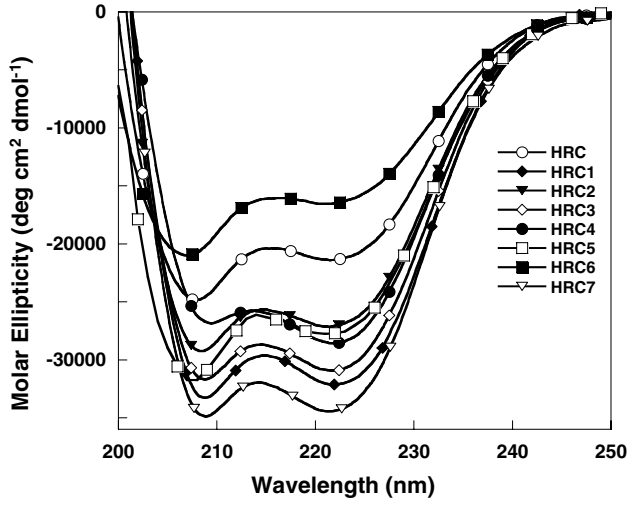

Fig. 3. CD analysis of helical structure of HRC analogs at 70 μM. Spectra were recorded in a 0.1 M KCl, 0.05 M PO_4 buffer, pH 7.

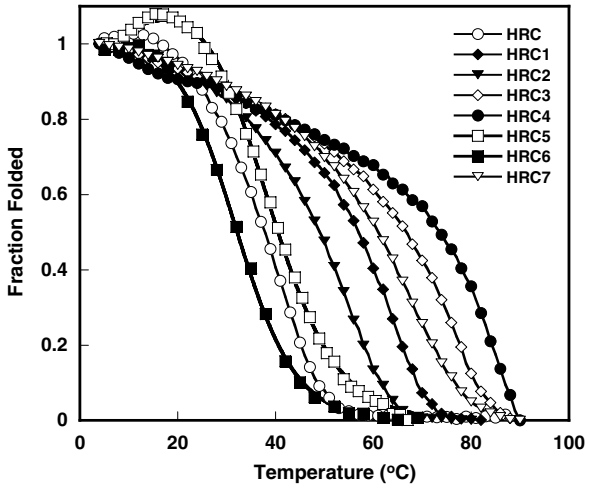

Fig. 4. Stability of HRC analogs. Temperature denaturation profiles of the HRC analogs monitored by CD at 222 nm in a 0.1 M KCl, 0.05 M PO_4 buffer, pH 7. Concentration was 70 μM. The fraction folded (f_f) of each peptide was calculated as $f_f = ([\theta] - [\theta]_u)/([\theta]_n - [\theta]_u)$, where $[\theta]$ is the observed mean residue molar ellipticity at 222 nm at any particular temperature, and $[\theta]_n$ and $[\theta]_u$ are the mean residue molar ellipticities at 222 nm of the native folded state at 4 °C and unfolded states, respectively.

Overall, the change in structure of HRC with substitutions was consistent with our design aim. That is the stability of the HRC1 coiled-coil increased due to the increase in hydrophobicity in the hydrophobic core by the Ala to Ile substitution at position 1172*a* (Fig. 1), as suggested by the hydrophobicity coefficients of all 20 amino acid residues in positions *a* and *d* of coiled-coils determined by Hodges and coworkers (Tripet et al., 2000; Wagschal et al., 1999a). Substitutions made to residues occurring in the b, c, and f heptad positions (the outer surface of the coiled-coil) with Ala, which has the highest α-helical propensity of all side-chains (Zhou et al., 1994), increased the α-helical structure and stability of HRC2 and HRC4 coiled-coils (Figs. 3 and 4, Table 1). The larger number of Ala substitutions in HRC4

substantially increased the stability relative to HRC2 (8 vs 2 Ala substitutions resulted in T_m values of 74 and 48 °C, respectively; Table 1). Peptide HRC3, which contained both the Ile residue in the hydrophobic core and the two Ala residues formed a more stable coiled-coil than either HRC1 and HRC2 analogs. A comparison of the substitutions showed that Ile resulted in a greater increase in coiled-coil stability than the two substituted Ala residues (ΔT_m HRC1–HRC was 21 °C compared to ΔT_m HRC2–HRC of 11 °C) indicating, as expected, that a single substitution in the hydrophobic core made a greater contribution to coiled-coil stability compared to two Ala substitutions in positions on the outer surface of the coiled-coil. However, the α-helical propensity effect for increasing stability can dominate over the increase in stability observed for the single Ala to Ile substitution in the hydrophobic core if the number of substitutions increasing α-helical propensity is large enough. That is, the 8 Ala substitutions (HRC4) increased stability by 37 °C (ΔT_m HRC4–HRC) compared to the single Ile substitution in the hydrophobic core (ΔT_m HRC1–HRC) of 21 °C.

The formation of the lactam bridge on the outer face of each helix significantly stabilized the coiled-coil of HRC5 compared to the non-covalent salt bridge in HRC6 (T_m of 32 °C for HRC6 compared to a T_m of 41 °C for HRC5; Fig. 4 and Table 1). Intrachain electrostatics also modulated stability of helical structure. Substitutions in HRC6 introduced an intrachain i to $i+4$ ionic attraction between E1156 and K1160 that was expected to increase α-helical structure and stability. However, K1160 also introduces two potential i to $i+3$ charge repulsions with R1157 and K1163 which could dominate over the introduced attraction. Thus, HRC6 which was destabilized relative to HRC (ΔT_m of 5 °C) was a control peptide for the covalent lactam bridge peptide HRC5. When a series of intrachain i to $i\pm3$ and i to $i\pm4$ salt bridges were introduced into HRC, the resulting analog HRC7 (Fig. 1) had a stability of 61 °C compared to HRC6 with the single salt bridge addition (T_m 32 °C) or HRC (T_m 37 °C) (Table 1).

The oligomerization state of these analogs was determined by size-exclusion chromatography (SEC) and shown to be either trimers or tetramers (Table 1). The oligomerization specificity of coiled-coils can be switched by even a single substitution, e.g., HRC (trimer) is switched to HRC1 (tetramer) by A1172I substitution.

3.3. Interaction of HRC analogs with HRN

3.3.1. Circular dichroism analysis

We used CD to analyze the ability of these HRC analogs to bind HRN. The results (Table 2) showed that interaction with HRN induces a significant change in α-helical conformation (e.g., HRN + HRC5, shown in Fig. 5), as compared with a theoretical spectrum obtained by summing experimental spectra of equivalent amounts of HRN and HRC analogs alone. These results suggested that HRC and analogs HRC1, 2, 3, 5, and 6 interact with HRN, whereas HRC4 and 7 have weak or no interaction (Table 2).

To test the stability of complexes of HRN with HRC analogs, 1:1 molar equivalent complexes of HRN and HRC or HRC analogs were determined by increasing temperature, as illustrated in Fig. 6. The results show that HRC (native sequence) can form a very stable complex with HRN, which agrees with our choice of the HRC sequence (1150–1185) as the key region of interaction with HRN and is suitable for substitutions to design analogs with improved properties.

A shown in Table 2, the substitutions resulted in a set of HRC analogs that form a set of HRC/HRN complexes with T_m values ranging from 59 to 88 °C compared to HRN alone with a T_m of 43 °C, except for HRC7 where the T_m of the mixture with HRN was similar to HRN or HRC7 alone, indicating that HRC7 does not interact with HRN (Fig. 6). Native HRC interacted and formed a more stable

Table 2
Summary of interaction of HRC analogs with HRN

Complex	$[\theta]_{222}$		Change in $[\theta]_{222}$	T_m[b] (°C)	ΔT_m[c]		Complex formation tested by		SPR binding test[e]
	Theoretical[a]	Observed			HRN	HRN−HRC	Native-PAGE[d]	SEC-HPLC[d]	
HRN		−20 890		43					
HRN−HRC	−15 920	−19 060	3140	85	+42	0	+	+	+
HRN−HRC1	−23 790	−25 340	1540	74	+31	−11	+	+	+
HRN−HRC2	−19 060	−23 070	4010	86	+43	+1	+	+	+
HRN−HRC3	−24 250	−26 130	1880	75	+32	−10	+	+	+
HRN−HRC4	−25 610	−26 180	570	59	+16	−26	−	+	+
HRN−HRC5	−22 420	−27 700	5280	88	+45	+3	+	+	+
HRN−HRC6	−15 980	−21 180	5200	83	+40	−2	+	+	+
HRN−HRC7	−23 340	−23 850	510	44	+1	−41	−	−	−

[a] The theoretical molar ellipticity for two non-interacting peptides was calculated by summing the two individual spectra.

[b] T_m is the transition midpoint temperature at which there is a 50% decrease in molar ellipticity $[\theta]_{222}$ compared with the fully folded peptide as determined by CD at 5 °C. The CD test was carried out after incubating the peptide mixture for 20 min at 5 °C. Concentration of each peptide was 7 μM.

[c] ΔT_m is the change in T_m from the T_m of HRN or the T_m of HRN−HRC complex.

[d] HRC peptides were incubated with HRN for 20 min, and then analyzed by Native-PAGE and SEC-HPLC. Concentration of each peptide in the mixture was 100 μM.

[e] SPR binding analysis was carried out on the CM5 sensor chip with the immobilization of the HRN trimer peptide (see Section 2).

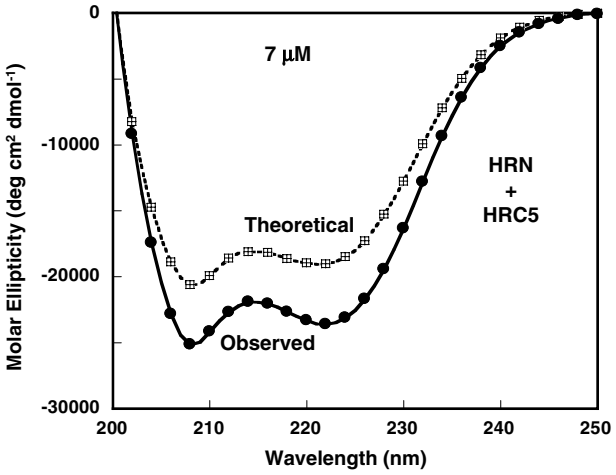

Fig. 5. CD analysis of the interaction of HRN and HRC5. CD spectrum of a 1:1 molar complex between HRN and HRC5 at 25 °C in a 0.1 M KCl, 0.05 M PO_4 buffer, pH 7. Peptide concentrations were 7 μM. The theoretical spectrum for two non-interacting peptides is shown for comparison, which was generated by adding the individual peptide spectra at the same concentrations.

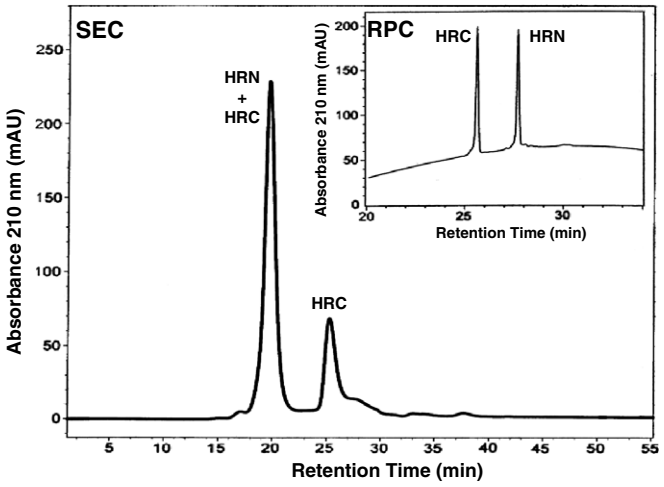

Fig. 7. SEC analysis of the HRN and HRC complex. HRN (2 nmol) and HRC (2 nmol) were pre-incubated together for 30 min in running buffer and then 10 μl of incubated sample was applied to SEC; conditions shown in Section 2.3. The absorbance peak at 19.7 min corresponding to the HRN/HRC complex was collected and subsequently analyzed by RP-HPLC (inset); Conditions shown in Section 2.3. Each absorbance peak is labeled accordingly.

complex with HRN than peptide analogs HRC1, HRC3, and HRC4. However, analogs HRC2, HRC5, and HRC6 formed complexes as stable as or slightly more stable than native HRC/HRN. HRN/HRC5 complex was not completely unfolded, even at 95 °C (Fig. 6).

3.3.2. Size-exclusion chromatography (SEC) analysis

To show complex formation between HRN and HRC analogs, we collected the earlier eluted peak from SEC and resolved it by RP-HPLC (Fig. 7). As shown in Table 2, except for HRC7, the other HRC analogs form stable complexes with HRN. The elution volumes of all the complexes, relative to *M*r standards, gave an apparent M_r of 27 490 Da, in good agreement with the M_r (27 900–28 340 Da) expected for a hexameric complex, formed by three molecules of HRN and three molecules of HRC or HRC analogs.

As shown in Fig. 7 (inset), the integrated peak areas converted to concentration using standard curves showed that the two peaks of HRN and HRC were in a 1:1 mole ratio as determined by RP-HPLC.

3.3.3. Native-polyacrylamide gel-electrophoresis (PAGE) analysis

To verify further complex formation between HRN and HRC analogs, we analyzed their interaction by Native-PAGE. The results are shown in Fig. 8 and Table 2. HRC or HRC analogs alone showed a band in the lower part of the gel. With the exception of HRC4 and HRC7, the mixture of HRC analogs and HRN showed two bands: the lower band had the same position as isolated HRC analog,

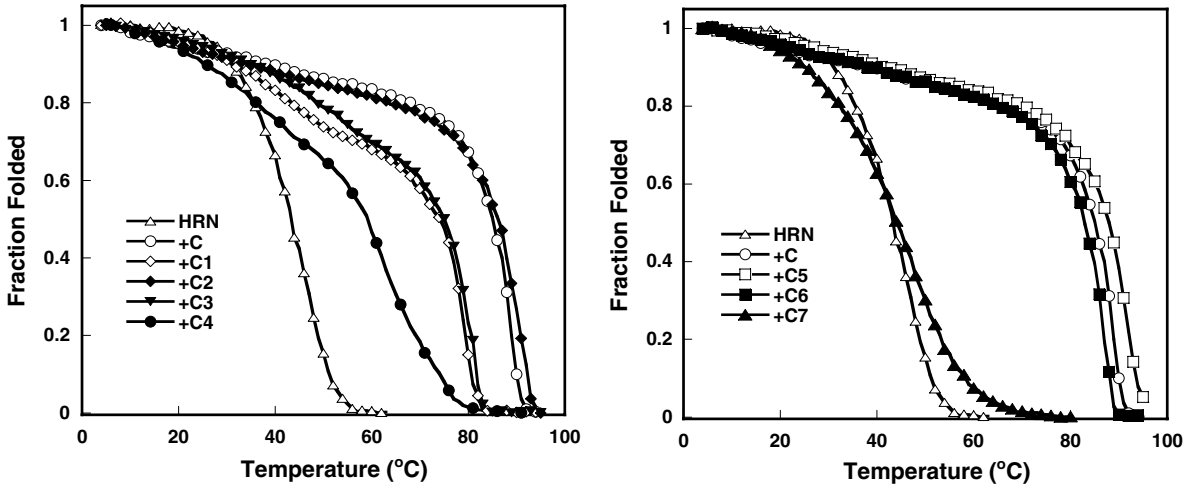

Fig. 6. Temperature denaturation profiles of HRN alone and a 1:1 molar mixture of HRN with HRC analog monitored by CD at 222 nm in a 0.1 M KCl, 0.05 M PO_4 buffer, pH 7. Concentrations of peptides were 7 μM. Fraction folded was calculated as described in Fig. 4 legend.

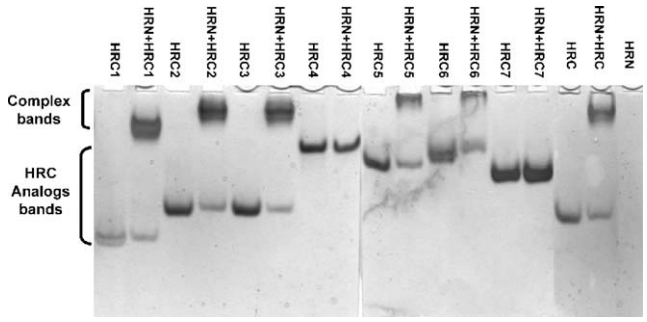

Fig. 8. Complex formation between HRC analogs and HRN, as determined by Native-PAGE. HRN and HRC analogs on their own or as pre-incubated equimolar (200 μM of each peptide) mixture were subjected to 15% PAGE. Samples were incubated for 30 min in 0.1 M KCl, 0.05 M PO_4 buffer, pH 7, diluted 1:1 (v/v) with native sample buffer and loaded onto the gel.

and the upper band is higher order oligomeric complex formed by HRN and HRC analog. HRN alone showed no band because it carries a net positive charge under the native gel electrophoresis conditions, and consequently does not enter the gel.

3.3.4. Surface plasmon resonance analysis of HRC analogs binding HRN

We next carried out SPR binding analysis of these HRC analogs on BIACORE chips with the immobilization of HRN trimer peptide. As shown in Fig. 9 and Table 2, with the exception of HRC7, HRC, and HRC analogs could bind the HRN trimer chip, which is consistent with the results from SEC analysis. The regeneration step for the chip surface required the use of a strong denaturant (6 M guanidine hydrochloride in 20 mM glycine, pH 2.0 for 1 min). This treatment also showed HRC analogs bind the HRN trimer very strongly.

Based on the results in Table 2 obtained from CD, SEC, Native-PAGE, and SPR analysis, compared to native HRC, the following results were obtained: HRC2 and HRC5 have high affinity for HRN; HRC1 and HRC3 showed decreased interaction with HRN and HRC4 could only form a weak complex with HRN. All the data showed no interaction between HRC7 and HRN. The results illustrate that when substitutions increase the stability of HRC helical structure (Table 1), such as that seen for HRC1, HRC3, and HRC4 (Table 2), the stability of the complex with HRN decreases. Therefore, the binding affinity of the analogs for HRN does not show a clear correlation to the coiled-coil stability of the HRC analogs. Even though HRC and HRC6 (Table 1) are only partially folded α-helical structures at the concentration of 7 μM, they can form very stable complexes with HRN (T_m of 85 and 83 °C, respectively, Table 2).

In this study, the HRC sequence was shortened to 28 residues (1158–1185) and 25 residues (1161–1185). The results in Table 3 showed that the 28-residue peptide had a much weaker interaction with HRN (a complex with a T_m of 58 °C) than the 36-residue HRC (1150–1185) (a complex with a T_m of 85 °C). When shortened to 25 residues (1161–1185), this analog showed no interaction with HRN. Even after formation of one lactam bridge was made in the core of the 25-residue HRC peptide to stabilize α-helical structure, it still did not show any interaction with HRN. This result is in good agreement with the previous reports (Bosch et al., 2004; Ingallinella et al., 2004; Zhu et al., 2004).

3.4. Interaction of HRC analogs with HRC

3.4.1. CD analysis

As shown in Fig. 4 and Table 1, the stability of most HRC analogs increased in comparison to the native HRC. One can propose that even though these HRC analogs are

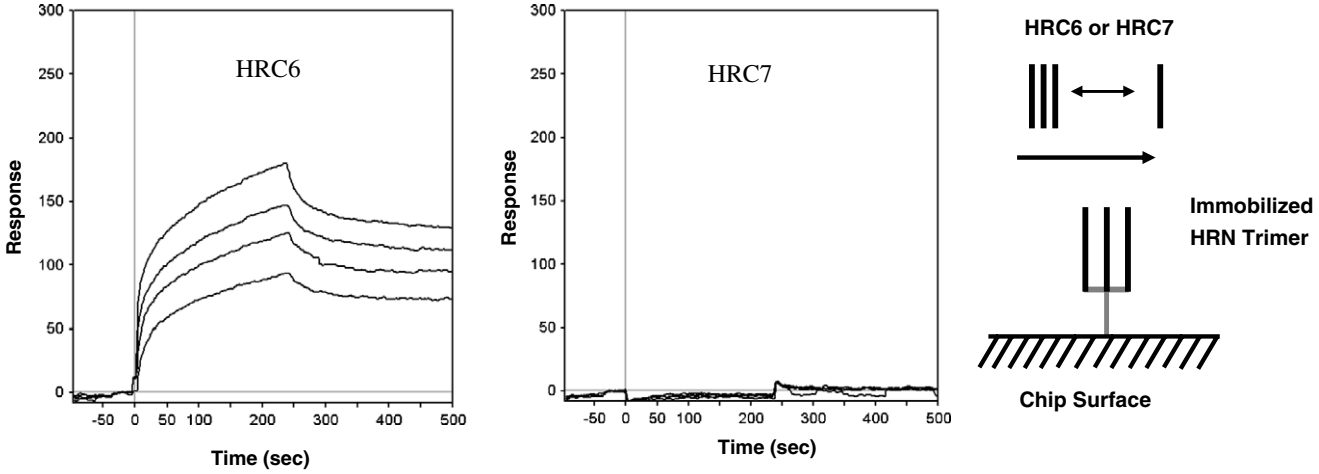

Fig. 9. Surface plasmon resonance analysis of the interaction of HRC6 and HRC7 with a HRN trimer chip. HRN trimer was covalently coupled to the Biacore CM5 chip surface. Binding experiments were performed at 25 °C in PBS buffer, pH 7.4, with 0.005% Tween 20. The peptides to be tested were introduced at four serial concentrations (5, 10, 20, and 50 μM) in running buffer in 80 μl injection volumes and at a flow rate of 20 μl/min, followed by 6 min of dissociation. The schematic shows HRC6 or HRC7 as a monomer-trimer equilibrium in solution when flowing over the immobilized HRN trimer on the chip surface.

Table 3
The structure of short HRC analogs and their interaction with HRN[a]

Short HRC analogs	Sequence	α-Helical structure	Interaction with HRN			
			CD	Native-PAGE	SEC	T_m (°C)
HRC 25	Ac-IQKEIDRLNEVAKNLNESLIDLQEL-amide	No	–	–	–	–
HRC 28	Ac-VVNIQKEIDRLNEVAKNLNESLIDLQEL-amide	No	+	+	+	58 °C
HRC5 25	Ac-IQKEI**E**RLN**K**VAKNLNESLIDLQEL-amide	Yes	–	–	–	–

[a] The conditions for CD, Native-PAGE, and SEC were the same as shown in Table 2.

more stable than HRC, they could still interact with native HRC to form mixed oligomers and thus prevent the formation of the hexameric complex between native HRC and HRN. To verify this assumption, we first used CD to analyze the interaction of these HRC analogs with native HRC. The results in Table 4 showed that the change in helical structure is induced by the interaction of HRC analogs with HRC, which suggested that HRC analogs HRC1, 2, 3, 4, and 5 interact with native HRC, whereas HRC6 and 7 have weak or no interaction.

To test if HRC analogs can stabilize HRC structure, temperature denaturation profiles were determined for a 1:1 mixture of HRC and HRC analogs. The results are illustrated in Fig. 10, and T_m values are shown in Table 4.

Table 4
Interaction of HRC analogs with HRC

Complex name	$[\theta]_{222}$		Change in $[\theta]_{222}$	T_m[b] (°C)	Interaction tested by Native-PAGE[c]	SPR binding test[d]
	Theoretical[a]	Observed				
HRC		12 320		5		
HRC–HRC1	−19 650	−25 240	5590	41	*ND*	+
HRC–HRC2	−11 090	−16 280	5190	34	+	+
HRC–HRC3	−19 000	−26 840	7840	46	+	+
HRC–HRC4	−20 600	−25 120	4520	55	+	+
HRC–HRC5	−18 470	−21 790	3320	38	+	+
HRC–HRC6	−9240	−10 610	1370	5	–	+
HRC–HRC7	−18 700	−20 280	1580	42	–	–

[a] The predicted molar ellipticity for two non-interacting peptides was calculated by summing the two individual spectra.
[b] T_m is the transition midpoint temperature at which there is a 50% decrease in molar ellipticity $[\theta]_{222}$ compared with the fully folded peptide as determined by CD. Concentration for each peptide was 7 μM. The CD determination was carried out after incubating the peptide mixture for 20 min at 4 °C.
[c] HRC analogs were incubated with native HRC for 20 min, and then analyzed by Native-PAGE. Concentration of each peptide for forming complexes was 100 μM. *ND* denotes that the interaction between HRC and HRC1 could not be determined by this method since these two peptides show the same mobility in gel-electrophoresis.
[d] SPR binding analysis was carried out on a CM5 chip with the immobilization of HRC trimer peptide (see Section 2).

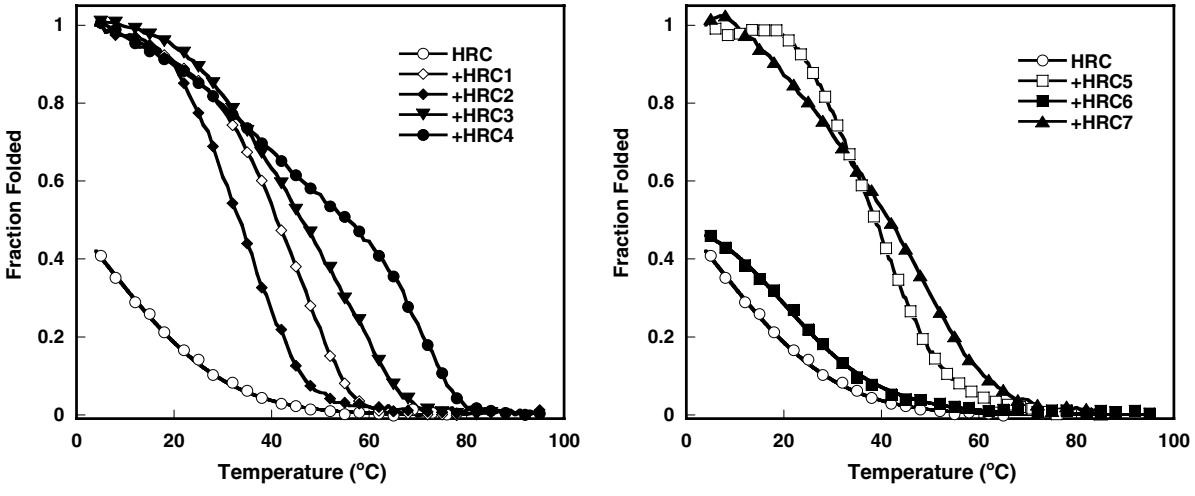

Fig. 10. Temperature denaturation profiles of HRC alone and a 1:1 molar mixture of HRC with HRC analog monitored by CD at 222 nm in a 0.1 M KCl, 0.05 M K_2HPO_4 buffer, pH 7. Peptide concentrations were 7 μM. Fraction folded was calculated as described in Fig. 4 legend.

These results show that HRC3 and HRC4 had the strongest interaction with HRC. Thus, the substitutions resulted in a set of HRC analogs that interact with native HRC with a set of T_m values ranging from 34 to 55 °C compared to the stability of HRC alone with a T_m of 5 °C. The T_m for the HRC6 and HRC mixture is similar to native HRC, suggesting no interaction with HRC.

3.4.2. Native-PAGE analysis

In the gel-shift experiment, the complex formation of HRC with HRC analogs was observed on native gel-electrophoresis to compare with the HRC and HRC analogs alone as shown in Fig. 11 and Table 4. HRC or HRC analogs alone showed a single band. With the exception of HRC1, HRC6, and HRC7, the mixture of HRC analogs and HRC showed smeared bands between the positions of the two bands of native HRC and HRC analog. These smeared bands may be caused by the equilibrium between bound and unbound and various combinations of HRC and HRC analog (3:0, 1:2, 2:1, and 0:3, respectively) would have different mobilities due to different mass/charge ratio. HRC1 and HRC showed the same mobility in the gel; thus, the interaction between them could not be determined by this method. However, the mixture of HRC and HRC6 or HRC7 showed two single bands corresponding to HRC and HRC6 or HRC7 alone, which suggests no interaction between HRC and HRC6 or HRC and HRC7 (Fig. 11).

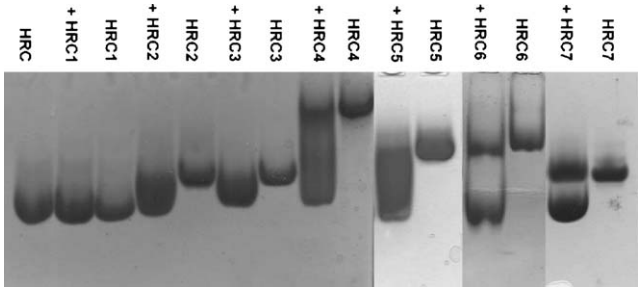

Fig. 11. Native-PAGE analysis of interaction of HRC analogs with HRC. HRC and HRC analogs on their own or as pre-incubated equimolar (200 μM of each peptide) mixture were subjected to 15% PAGE. Samples were incubated for 30 min in 0.1 M KCl, 0.05 M PO_4 buffer, pH 7, and the diluted 1:1 (v/v) with native sample buffer and loaded onto the gel.

3.4.3. Surface plasmon resonance analysis of HRC analogs binding HRC

We have carried out SPR binding analysis of these HRC analogs on BIACORE chip with the immobilization of HRC trimer peptide. As shown in Fig. 12 and Table 4, except for HRC7, HRC, and HRC analogs could bind the HRC trimer chip, which is consistent with native-PAGE analysis.

Based on the results in Table 4 obtained from CD, the complex stability order of HRC/HRC analogs is HRC4> HRC3> HRC7 ≈ HRC1> HRC5>HRC2>HRC≈ HRC6. All analogs showed interaction with HRC by native gel electrophoresis and SPR analysis, except for HRC7. HRC6 showed very weak interaction with HRC since the complex has similar helical structure and stability ($T_m = 5$ °C) to native HRC. Therefore, the interaction of the analogs with native HRC correlates with stability, except for HRC7.

4. Discussion

Formation of the six-helix bundle is a critical conformational change of the S protein during fusion of the SARS-CoV and target cell membranes. Clearly therefore, the functional domains of the S protein involved in membrane fusion represent attractive targets for the discovery of viral entry inhibitors of SARS-CoV. A compound that blocks the S protein six-helix bundle formation may be a potent SARS-CoV fusion inhibitor. Therefore, determination of S protein six-helix bundle formation is important for studying the mechanism by which SARS-CoV induces

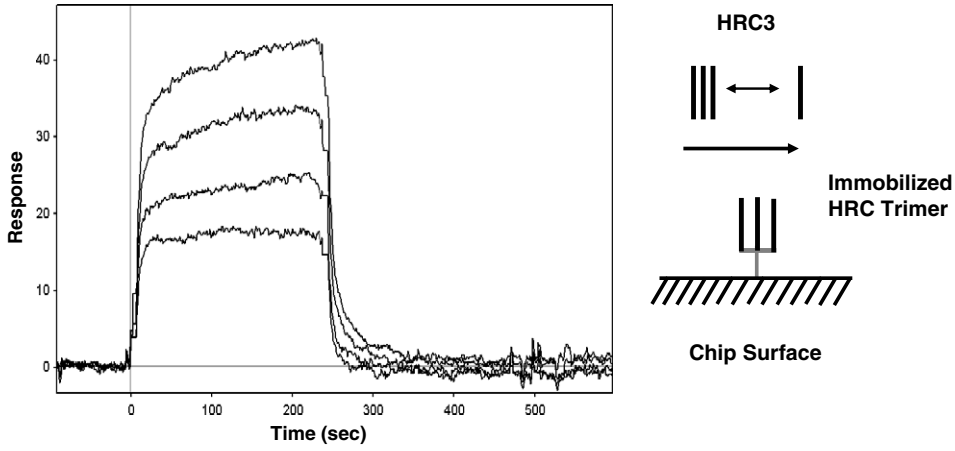

Fig. 12. Surface plasmon resonance analysis of the interaction of HRC3 with HRC trimer chip. HRC trimer was covalently coupled to the Biacore CM5 chip surface. Binding experiments were performed at 25 °C in PBS buffer, pH 7.4, with 0.005% Tween 20. The peptides to be tested w ere introduced at four serial concentrations (5, 10, 20, and 50 μM) in running buffer in 80 μl injection volumes and at a flow rate of 20 μl/min, followed by 6 min of dissociation. HRC3 is shown in the schematic as a monomer-trimer equilibrium in solution when flowing over the immobilized HRC trimer on the chip surface.

membrane fusion and for identification of SARS-CoV fusion effective inhibitors targeting S protein. In this biophysical study, we made substitutions to HRC and studied their effect on α-helical structure and stability in the absence and presence of the native sequences of HRN and HRC.

In the crystallographic structures of the six-helix bundle conformation (Duquerroy et al., 2005; Supekar et al., 2004; Xu et al., 2004a), the 49 residues (902–950) in the HRN region and the 36 residues (1150–1185) in the HRC region were identified to be the major binding regions for their interactions. Interestingly, the 36-residue length of HRC matches the 49 residues of HRN in a trimeric coiled-coil conformation. This is accomplished by residues 1161–1175 in HRC forming a 5-turn α-helix with residues 1150–1160 at the N-terminus and residues 1176–1185 at the C-terminus of HRC forming two extended conformations. This result suggests the N- and C- terminal residues of HRC must be able to readily change conformation from an α-helical conformation in a trimeric coiled-coil to the extended conformation when bound to HRN in the six-helix bundle conformation.

Substitutions in the region of HRC could have one of three effects on its interaction with HRN: first, substitution of a particular native residue could affect the interaction of that side-chain with HRN, thus decreasing the stability of the HRN/HRC complex; second, substitution could stabilize the α-helical conformation in HRC which in turn would reduce the ability of the N- and/or C-terminal regions of HRC to readily change conformation from α-helical to extended on interacting with HRN; third, if the monomeric form of HRC is the interacting species with HRN, then substitutions that stabilize the oligomeric structure would shift the monomer–oligomer equilibrium in the favor of the oligomer and at some point no monomer would be available to interact with HRN.

In our analysis of the interaction between HRC and HRN, we used the X-ray crystallographic structure of the six-helix bundle conformation of Supekar et al. (2004) (pdb accession number is 1BEZ) and for the interactions in HRC we used the solution NMR structure of residues 1141–1193 by Hakansson-McReynolds et al. (2006) (pdb accession number 2FXP). Our choice of the HRC region for inhibitor design (HRC 1150–1185) was initially based on our biophysical studies (Tripet et al., 2004) before any three-dimensional structural information was available. This choice was confirmed by the NMR solution structure which showed that the trimeric coiled-coil was stabilized by a hydrophobic core involving hydrophobic residues in the *a* and *d* positions from Ile 1151*a* to Leu 1182*d* (Fig. 1). The NMR structure also showed the importance of Leu 1185*g* in hydrophobic packing between the three polypeptide chains. The importance of hydrophobes in positions *e* and *g* of coiled-coils for increasing coiled-coil stability has been previously documented by biophysical studies and the X-ray crystallographic structure of a cortexillin I/GCN4 hybrid coiled-coil (Lee et al., 2003).

In the six-helix bundle conformation the interaction between HRC and HRN can be divided into three regions based on HRC (Fig. 1). Region 1 involves residues 1150–1160 of HRC which are helical in the prefusion state (NMR solution structure of the HRC trimer) and extended in the 6-helix bundle conformation. That is, in this region hydrophobes Ile 1151*a*, Ile 1154*d*, and Val 1158*a* are in the hydrophobic core in the pre-fusion state and hydrophobe Val 1159*b* is exposed on the outside of the trimeric coiled-coil of HRC. In contrast, in the six-helix bundle conformation Val 1159*b* is now buried along with Ile 1151*a* and Ile 1154*d* on interaction with HRN and Val 1158*a* is now exposed. That is, there has been a switch of hydrophobes between the two states involving Val 1158*a* and Val 1159*b*. Region 2 involves residues 1161–1175 which are helical in both the prefusion state (HRC trimeric state) and the six-helix bundle conformation and the same four hydrophobes (Ile 1161*d*, Ile 1165*a*, Leu 1168*d*, and Leu 1175*d*) are stabilizing this helical structure in both states (interacting with the other chains of the HRC trimer or interacting with the HRN trimer). In this region there is also one hydrophobe not in the *a* and *d* positions, Val 1171*g*, which is interacting to stabilize the hydrophobic core in the HRC trimer and is also involved in the interaction with HRN. This residue is conserved as a hydrophobe in all coronaviruses as Val, Leu or Ala (Duquerroy et al., 2005). Region 3 involves residues 1176–1185 of HRC which are helical in the HRC trimer and extended in the six-helix bundle conformation. That is, hydrophobes Leu 1179*a*, Leu 1182*d*, and Leu 1185*g* are in the hydrophobic core of the HRC trimer and Ile1180*b* is exposed on the outside of the trimeric coiled-coil of HRC. In contrast, in the six-helix bundle conformation Ile 1180*b* is now buried along with Leu 1182*d* on interaction with HRN, and Leu 1179*a* is now exposed (Leu 1185*g* is not present in the crystal structure of the six-helix bundle). That is, there has been a switch of hydrophobes between the two states involving residues Leu 1179*a* and Ile 1180*b*. It is interesting that the two hydrophobes, Val 1159*b*, and Ile 1180*b* that are surface exposed in the HRC trimer and buried on interaction with HRN in the six-helix bundle conformation are conserved among all coronaviruses as a hydrophobe (Val or Leu at position 1159 and a β-branched hydrophobe Val or Ile at position 1180), indicating their importance to presumably stabilize the six-helix bundle conformation (Duquerroy et al., 2005).

The question to be addressed is whether we can explain the behaviors of our HRC analogs in light of the structural information. A HRC inhibitor could inhibit six-helix bundle formation in several ways: by binding to native HRC, by binding to native HRN or by interacting with both regions. The requirement for the complete HRC sequence 1150–1185 for binding to HRN was demonstrated by our deletion analogs (Table 3). The importance of the N-terminal region of HRC to interact with HRN was demonstrated by the 25-residue peptide (HRC 25) which had 11 residues (1150–1160) deleted from HRC was unable to interact with HRN. Adding back 3 additional residues (VVN, residues

1158–1160) to HRC 25 produced HRC 28 which bound to HRN with a T_m value for the HRC/HRN complex of 58 °C, compared to the stability of HRN-HRC complex of 85 °C (Table 2). This result illustrates that the N-terminal seven residues (1150–1157) are extremely important for HRC binding to HRN. In particular, based on the X-ray structure of the six-helix bundle Ile 1151 or Ile 1154 interact with HRN in the hydrophobic core as discussed above. Similarly, truncation of the N-terminal residues 1150–1160 from the HRC5 sequence (Fig. 1), the best binding analog to HRN (Table 2) also showed no interaction with HRN. This result is also supported by Duquerroy et al. (2005), who reported that the extended regions of HRC consolidate their interaction with HRN by a string of asparagine and glutamine side chains from the HRN coiled-coil, which hydrogen bond to the HRC main chain. This extensive hydrogen-bonding network zips the HRC chain along the HRN interhelical grooves.

Four HRC analogs (HRC1, HRC2, HRC3, and HRC4, Fig. 1) were designed to increase α-helical structure and stability of the α-helix and resulting coiled-coil by either substitution of residues in positions *b*, *c*, and *f* of the heptad repeat by Ala (outer positions on the coiled-coil) to increase α-helical propensity or substitution of Ala by Ile in position *a* to increase hydrophobicity in the hydrophobic core. The order of stability of these analogs was HRC2 < HRC1 < HRC3 < HRC4 (Table 1). Interestingly, this identical order was obtained for the stability of 1:1 mixtures of these analogs with HRC (Table 4). These results suggest that increasing the stability of the HRC analogs increases their ability to interact with the native HRC sequence. The most stable analog of this series of analogs was HRC4 with a T_m of 74 °C compared to HRC with a T_m of 37 °C at a peptide concentration of 70 μM (Table 1). Thus, this dramatic increase in stability does not prevent interaction with HRC and suggests that the stability of this HRC analog is not so high as to prevent interaction with the native HRC sequence whether the interaction is based on the oligomeric coiled-coil or monomer of the analog interacting with the native HRC sequence.

Interestingly, HRC and three HRC analogs that are the least stable oligomeric coiled-coils (T_m values of 37, 48, 41, and 32 °C for HRC, HRC2, HRC5, and HRC6, respectively, Table 1) formed the most stable complexes with HRN (T_m values of 85, 86, 88, and 83 °C for HRN complexes involving HRC, HRC2, HRC5, and HRC6, respectively, Table 2). These results suggest that you can increase the stability of the oligomeric form of HRC with little effect on the formation and stability of the HRN/HRC complex (11 °C increase in T_m from 37 °C for HRC to 48 °C for HRC2). On the other hand, the substitutions in HRC which stabilized the oligomeric coiled-coil structure the most (T_m values of 57, 66, and 74 °C for HRC1, HRC3, and HRC4, respectively compared to HRC with a T_m of 37 °C, Table 1) formed the least stable complexes with HRN (T_m values of 74, 75, and 59 °C, respectively, compared to HRC/HRN complex with a T_m of 85 °C, Table 2).

The substitutions that increase hydrophobicity in the hydrophobic core (Ala 1172 Ile) increased stability of the trimer (HRC1 and HRC3, Table 1) as expected. These two analogs also bind to native HRC (Table 4). However, this Ala to Ile substitution was disruptive to the stability of the HRN/HRC1 or HRN/HRC3 complex, compared to the native HRN/HRC complex (Table 2). Obviously, Ile is more ideal for stabilizing the trimer than Ala but Ala at this position is more ideal than Ile for stabilizing the HRN interaction. This suggests that though this region 2 (Fig. 1) is helical in the trimer and helical on interacting with HRN, the interactions between the helix and HRN are different from the helix-helix interactions in the trimer.

HRC5 has a i to $i+4$ covalent lactam bridge between Glu and Lys (Fig. 1) which did provide an increase in stability of the trimeric coiled-coil (compare the control peptide HRC6 with a salt bridge at the same positions with a T_m of 32 °C to HRC5 with a T_m of 41 °C). However, the substitutions of Asp and Glu in HRC to Glu and Lys in HRC6 suggest that Asp and Glu must be important for the stability of the trimeric coiled-coil of HRC since HRC6 was less stable than the native HRC sequence by 5 °C (Table 1). This clearly demonstrates that the covalent constraint does stabilize the α-helix and the interaction of HRC5 with HRC but that the location of the constraint should be such as to not disrupt the coiled-coil in the control peptide with the non-covalent ion-pair (HRC6). Thus, we probably did not achieve maximum benefit of this covalent constraint. Since HRC5 stabilized the complex with HRN more than any other analog (Table 4), HRC5 should be classified as a potential HRN-specific or combined HRN and HRC inhibitor. Thus, clearly stabilizing the α-helical region in the six-helix bundle state is advantageous.

In fact, HRC4 (8 Ala substitutions to increase α-helical propensity, Fig. 1) formed the most stable oligomeric coiled-coil of all the HRC analogs (T_m of 74 °C compared to 37 °C for native HRC, Table 1) and the least stable complex with HRN (T_m of 59 or 26 °C below the stability of the native HRN/HRC complex, Table 2). On the other hand, HRC4 formed the most stable complex with native HRC increasing the T_m by 50 °C (Table 4). These results can be explained based on structural information. Stabilizing the helix analog along the length of the trimeric coiled-coil provides an excellent potential inhibitor of the six-helix bundle state by complexing with native HRC (a potential HRC-specific inhibitor), but stabilizing region 1 and 3 (Fig. 1) in the helical conformation prevents the conformational change of these regions to go to the extended conformation in the six-helix bundle conformation. Also, we have substituted the two conserved residues Val 1159 and Ile 1180 with Ala and these residues are critical for interaction with HRN. Thus, HRC4 would not exert its inhibitory effect by binding to HRN.

HRC7, with 10 substitutions of Glu and Lys into the HRC sequence at positions *b*, *c*, *f*, and *g* to create a series of i to $i+3$ and i to $i+4$ intrachain electrostatic interactions (Fig. 1), did stabilize the α-helical structure of the trimer by

24 °C compared to native HRC (Table 1). CD results suggested an interaction of HRC7 and HRC (Fig. 10) but no interaction was observed by Native-PAGE (Fig. 11) or SPR (Table 4). Though these salt-bridges stabilize the coiled-coil structure, at least some of these side-chains in this analog must be critical for disrupting interactions with native HRC. Thus, the interaction with HRC requires more than just the packing of the *a* and *d* positions of the hydrophobic core which are identical in HRC7 and native HRC. In addition, HRC7 showed absolutely no binding to HRN. This can be explained by the fact that the 3 conserved hydrophobes in all coronaviruses (positions 1159, 1171, and 1178) that are important for binding to HRN have been substituted by charged residues which would disrupt and destabilize the interaction with HRN. Recently it was also reported that position 1160 is a conserved Asn/Asp residue in coronaviruses and from the structure of the six-helix bundle the side-chain hydrogen bonds to the polypeptide backbone of HRC and Glu 1164 is conserved for interaction with HRN via a salt bridge (Duquerroy et al., 2005). Therefore, the substitution of these five positions would be expected to abolish binding to HRN.

In summary, the above results show that increasing α-helical propensity of side-chains, increasing hydrophobicity in the hydrophobic core, increasing intrachain ionic interactions or addition of a covalent constraint that increase coiled-coil stability over the native sequence can be beneficial to the design of a potential peptide inhibitors that are HRC-specific (HRC1, HRC3, and HRC4) or inhibitors that can bind both HRC and HRN simultaneously (HRC2 and HRC5). Biological experiments will be carried out to verify the inhibitory activity of these potential peptide inhibitors and whether HRN or HRC is the better target.

Acknowledgments

This work was supported by National Institutes of Health Grant PO1-AI059576 and the John Stewart Chair in Peptide Chemistry (to R. S. H.). We thank Dziuleta Cepeniene for help with peptide synthesis. CD and BIACORE analysis were performed at the Biophysics Core Facility, University of Colorado at Denver and Health Sciences Center.

References

Bianchi, E., Finotto, M., Ingallinella, P., Hrin, R., Carella, A.V., Hou, X.S., Schleif, W.A., Miller, M.D., Geleziunas, R., Pessi, A., 2005. Covalent stabilization of coiled coils of the HIV gp41 N region yields extremely potent and broad inhibitors of viral infection. Proc. Natl. Acad. Sci. USA 102, 12903–12908.

Bosch, B.J., Martina, B.E., Van Der Zee, R., Lepault, J., Haijema, B.J., Versluis, C., Heck, A.J., De Groot, R., Osterhaus, A.D., Rottier, P.J., 2004. Severe acute respiratory syndrome coronavirus (SARS-CoV) infection inhibition using spike protein heptad repeat-derived peptides. Proc. Natl. Acad. Sci. USA 101, 8455–8460.

Bosch, B.J., van der Zee, R., de Haan, C.A., Rottier, P.J., 2003. The coronavirus spike protein is a class I virus fusion protein: structural and functional characterization of the fusion core complex. J. Virol. 77, 8801–8811.

Chakrabartty, A., Kortemme, T., Baldwin, R.L., 1994. Helix propensities of the amino acids measured in alanine-based peptides without helix-stabilizing side-chain interactions. Protein Sci. 3, 843–852.

Chan, D.C., Chutkowski, C.T., Kim, P.S., 1998. Evidence that a prominent cavity in the coiled coil of HIV type 1 gp41 is an attractive drug target. Proc. Natl. Acad. Sci. USA 95, 15613–15917.

Chan, D.C., Kim, P.S., 1998. HIV entry and its inhibition. Cell 93, 681–684.

Duquerroy, S., Vigouroux, A., Rottier, P.J., Rey, F.A., Bosch, B.J., 2005. Central ions and lateral asparagine/glutamine zippers stabilize the post-fusion hairpin conformation of the SARS coronavirus spike glycoprotein. Virology 335, 276–285.

Eckert, D.M., Kim, P.S., 2001a. Design of potent inhibitors of HIV-1 entry from the gp41 N-peptide region. Proc. Natl. Acad. Sci. USA 98, 11187–11192.

Eckert, D.M., Kim, P.S., 2001b. Mechanisms of viral membrane fusion and its inhibition. Annu. Rev. Biochem. 70, 777–810.

Guan, Y., Zheng, B.J., He, Y.Q., Liu, X.L., Zhuang, Z.X., Cheung, C.L., Luo, S.W., Li, P.H., Zhang, L.J., Guan, Y.J., Butt, K.M., Wong, K.L., Chan, K.W., Lim, W., Shortridge, K.F., Yuen, K.Y., Peiris, J.S., Poon, L.L., 2003. Isolation and characterization of viruses related to the SARS coronavirus from animals in southern China. Science 302, 276–278.

Hakansson-McReynolds, S., Jiang, S., Rong, L., Caffrey, M., 2006. Solution structure of the SARS-coronavirus HR2 domain in the prefusion state. J. Biol. Chem. 281, 11965–11971.

Hartley, D.M., Smith, D.L., 2003. Uncertainty in SARS epidemiology. Lancet 362, 170–171.

Holmes, K.V., 2005. Structural biology. Adaptation of SARS coronavirus to humans. Science 309, 1822–1823.

Houston Jr., M.E., Gannon, C.L., Kay, C.M., Hodges, R.S., 1995. Lactam bridge stabilization of alpha-helical peptides: ring size, orientation and positional effects. J. Pept. Sci. 1, 274–282.

Houston Jr., M.E., Wallace, A., Bianchi, E., Pessi, A., Hodges, R.S., 1996. Use of a conformationally restricted secondary structural element to display peptide libraries: a two-stranded alpha-helical coiled-coil stabilized by lactam bridges. J. Mol. Biol. 262, 270–282.

Ingallinella, P., Bianchi, E., Finotto, M., Cantoni, G., Eckert, D.M., Supekar, V.M., Bruckmann, C., Carfi, A., Pessi, A., 2004. Structural characterization of the fusion-active complex of severe acute respiratory syndrome (SARS) coronavirus. Proc. Natl. Acad. Sci. USA 101, 8709–8714.

Kates, S.A., Daniels, S.B., Albericio, F., 1993. Automated allyl cleavage for continuous-flow synthesis of cyclic and branched peptides. Anal. Biochem. 212, 303–310.

LaBonte, J., Lebbos, J., Kirkpatrick, P., 2003. Enfuvirtide. Nat. Rev. Drug Discov. 2, 345–346.

Lee, D.L., Ivaninskii, S., Burkhard, P., Hodges, R.S., 2003. Unique stabilizing interactions identified in the two-stranded alpha-helical coiled-coil: crystal structure of a cortexillin I/GCN4 hybrid coiled-coil peptide. Protein Sci. 12, 1395–1405.

Li, F., Li, W., Farzan, M., Harrison, S.C., 2005. Structure of SARS coronavirus spike receptor-binding domain complexed with receptor. Science 309, 1864–1868.

Liu, S., Xiao, G., Chen, Y., He, Y., Niu, J., Escalante, C.R., Xiong, H., Farmar, J., Debnath, A.K., Tien, P., Jiang, S., 2004. Interaction between heptad repeat 1 and 2 regions in spike protein of SARS-associated coronavirus: implications for virus fusogenic mechanism and identification of fusion inhibitors. Lancet 363, 938–947.

Lu, M., Blacklow, S.C., Kim, P.S., 1995. A trimeric structural domain of the HIV-1 transmembrane glycoprotein. Nat. Struct. Biol. 2, 1075–1082.

Normile, D., 2004a. Infectious diseases. Mounting lab accidents raise SARS fears. Science 304, 659–661.

Normile, D., 2004b. Infectious diseases. Second lab accident fuels fears about SARS. Science 303, 26.

O'Neil, K.T., DeGrado, W.F., 1990. A thermodynamic scale for the helix-forming tendencies of the commonly occurring amino acids. Science 250, 646–651.

Root, M.J., Kay, M.S., Kim, P.S., 2001. Protein design of an HIV-1 entry inhibitor. Science 291, 884–888.

Skehel, J.J., Wiley, D.C., 2000. Receptor binding and membrane fusion in virus entry: the influenza hemagglutinin. Annu. Rev. Biochem. 69, 531–569.

Spaan, W., Cavanagh, D., Horzinek, M.C., 1988. Coronaviruses: structure and genome expression. J. Gen. Virol. 69 (Pt 12), 2939–2952.

Supekar, V.M., Bruckmann, C., Ingallinella, P., Bianchi, E., Pessi, A., Carfi, A., 2004. Structure of a proteolytically resistant core from the severe acute respiratory syndrome coronavirus S2 fusion protein. Proc. Natl. Acad. Sci. USA 101, 17958–17963.

Tripet, B., Howard, M.W., Jobling, M., Holmes, R.K., Holmes, K.V., Hodges, R.S., 2004. Structural characterization of the SARS-coronavirus spike S fusion protein core. J. Biol. Chem. 279, 20836–20849.

Tripet, B., Kao, D., Jeffers, S., Holmes, K., Hodges, R., 2006. Template-based HRC antigens elicit neutralizing antibodies to the SARS-CoV. J. Struct. Biol. (in press).

Tripet, B., Wagschal, K., Lavigne, P., Mant, C.T., Hodges, R.S., 2000. Effects of side-chain characteristics on stability and oligomerization state of a de novo-designed model coiled-coil: 20 amino acid substitutions in position "d". J. Mol. Biol. 300, 377–402.

Wagschal, K., Tripet, B., Hodges, R.S., 1999a. De novo design of a model peptide sequence to examine the effects of single amino acid substitutions in the hydrophobic core on both stability and oligomerization state of coiled-coils. J. Mol. Biol. 285, 785–803.

Wagschal, K., Tripet, B., Lavigne, P., Mant, C., Hodges, R.S., 1999b. The role of position *a* in determining the stability and oligomerization state of alpha-helical coiled coils: 20 amino acid stability coefficients in the hydrophobic core of proteins. Protein Sci. 8, 2312–2329.

Xu, Y., Lou, Z., Liu, Y., Pang, H., Tien, P., Gao, G.F., Rao, Z., 2004a. Crystal structure of severe acute respiratory syndrome coronavirus spike protein fusion core. J. Biol. Chem. 279, 49414–49419.

Xu, Y., Zhu, J., Liu, Y., Lou, Z., Yuan, F., Cole, D.K., Ni, L., Su, N., Qin, L., Li, X., Bai, Z., Bell, J.I., Pang, H., Tien, P., Gao, G.F., Rao, Z., 2004b. Characterization of the heptad repeat regions, HR1 and HR2, and design of a fusion core structure model of the spike protein from severe acute respiratory syndrome (SARS) coronavirus. Biochemistry 43, 14064–14071.

Yuan, K., Yi, L., Chen, J., Qu, X., Qing, T., Rao, X., Jiang, P., Hu, J., Xiong, Z., Nie, Y., Shi, X., Wang, W., Ling, C., Yin, X., Fan, K., Lai, L., Ding, M., Deng, H., 2004. Suppression of SARS-CoV entry by peptides corresponding to heptad regions on spike glycoprotein. Biochem. Biophys. Res. Commun. 319, 746–752.

Zhou, N.E., Kay, C.M., Hodges, R.S., 1994. The role of interhelical ionic interactions in controlling protein folding and stability. De novo designed synthetic two-stranded alpha-helical coiled-coils. J. Mol. Biol. 237, 500–512.

Zhu, J., Xiao, G., Xu, Y., Yuan, F., Zheng, C., Liu, Y., Yan, H., Cole, D.K., Bell, J.I., Rao, Z., Tien, P., Gao, G.F., 2004. Following the rule: formation of the 6-helix bundle of the fusion core from severe acute respiratory syndrome coronavirus spike protein and identification of potent peptide inhibitors. Biochem. Biophys. Res. Commun. 319, 283–288.